The potential impact of changes in lower stratospheric water vapour on stratospheric temperatures over the past 30 years

RMetS
Royal Meteorological Society

The potential impact of changes in lower stratospheric water vapour on stratospheric temperatures over the past 30 years

A. C. Maycock,[a]* M. M. Joshi,[b] K. P. Shine,[c] S. M. Davis[d,e] and K. H. Rosenlof[d]

[a]*Centre for Atmospheric Science, Department of Chemistry, University of Cambridge, UK*
[b]*School of Environmental Sciences, University of East Anglia, Norwich, UK*
[c]*Department of Meteorology, University of Reading, UK*
[d]*NOAA/ESRL/Chemical Sciences Division, Boulder, CO, USA*
[e]*CIRES, University of Colorado, Boulder, CO, USA*

*Correspondence to: A. C. Maycock, Centre for Atmospheric Science, Department of Chemistry, University of Cambridge, Cambridge, CB2 1EW, UK.
E-mail: acm204@cam.ac.uk

This study investigates the potential contribution of observed changes in lower stratospheric water vapour to stratospheric temperature variations over the past three decades using a comprehensive global climate model (GCM). Three case studies are considered. In the first, the net increase in stratospheric water vapour (SWV) from 1980–2010 (derived from the Boulder frost-point hygrometer record using the gross assumption that this is globally representative) is estimated to have cooled the lower stratosphere by up to ∼0.2 K decade^{-1} in the global and annual mean; this is ∼40% of the observed cooling trend over this period. In the Arctic winter stratosphere there is a dynamical response to the increase in SWV, with enhanced polar cooling of 0.6 K decade^{-1} at 50 hPa and warming of 0.5 K decade^{-1} at 1 hPa. In the second case study, the observed decrease in tropical lower stratospheric water vapour after the year 2000 (imposed in the GCM as a simplified representation of the observed changes derived from satellite data) is estimated to have caused a relative increase in tropical lower stratospheric temperatures by ∼0.3 K at 50 hPa. In the third case study, the wintertime dehydration in the Antarctic stratospheric polar vortex (again using a simplified representation of the changes seen in a satellite dataset) is estimated to cause a relative warming of the Southern Hemisphere polar stratosphere by up to 1 K at 100 hPa from July–October. This is accompanied by a weakening of the westerly winds on the poleward flank of the stratospheric jet by up to 1.5 m s^{-1} in the GCM. The results show that, if the measurements are representative of global variations, SWV should be considered as important a driver of transient and long-term variations in lower stratospheric temperature over the past 30 years as increases in long-lived greenhouse gases and stratospheric ozone depletion.

Key Words: temperature trends; stratosphere and climate; climate modelling; Antarctic dehydration; tropical stratosphere; polar stratosphere

Received 19 December 2012; Revised 10 September 2013; Accepted 28 October 2013; Published online in Wiley Online Library 21 February 2014

1. Introduction

The concentration of water vapour in the stratosphere has been shown to vary on interannual to multi-decadal time-scales. For example, it has been reported that there was a net increase in stratospheric water vapour (SWV) of ∼30% over the late twentieth century (Rosenlof, 2001), followed by a sudden drop of ∼15% after 2000 (Randel *et al.*, 2006). Such changes in SWV are thought to occur largely as a result of variations in tropical tropopause temperatures, which control the dehydration of air as it passes into the stratosphere (Mote *et al.*, 1996; Fueglistaler and Haynes, 2005) and/or changes in the production of SWV from methane oxidation (Le Texier *et al.*, 1988). As a radiatively active species, changes in SWV may affect stratospheric temperatures (Maycock *et al.*, 2011) and global-mean radiative forcing (Forster and Shine, 2002), which can subsequently impact on the large-scale atmospheric circulation (Maycock *et al.*, 2013).

Observations indicate that the lower stratosphere cooled by ∼0.5 K decade^{-1} in the global mean between 1979 and 2007 (Randel *et al.*, 2009b). Although stratospheric cooling is expected in response to increases in atmospheric carbon dioxide and

[The copyright in this article was changed on 27 November 2014 after original publication.]

stratospheric ozone depletion, it is plausible that changes in SWV may also have contributed to observed temperature trends. A key limitation in quantifying this effect is the paucity of long-term global observations of SWV. Forster and Shine (1999) assumed a globally uniform increase of 0.7 ppmv as an approximation of the 1979–1997 SWV trend. They used an intermediate complexity global climate model (GCM) to show that the assumed change in SWV had the greatest impact on temperatures in the lower stratosphere, with an annual-mean cooling at 50 hPa of $\sim$0.4 K decade^{-1} in the Tropics and 0.8–1.3 K decade^{-1} in the polar regions. Shine *et al.* (2003) estimated the global-mean cooling due to the increase in SWV over a similar period to be 0.1–0.2 K decade^{-1} in the upper stratosphere, but found large uncertainties in the lower stratosphere across a number of models. This was partly because the individual modelling groups who carried out calculations had assumed different SWV trends. However, it is also likely to be partly due to fundamental differences in the representation of SWV in broad-band radiation codes (Oinas *et al.*, 2001; Maycock and Shine, 2012).

The goal of this study is to quantify the potential contribution of changes in lower stratospheric water vapour to seasonal and longer-term stratospheric temperature variations over the past three decades. We limit our attention to the lower stratosphere, because this is where SWV has been observed best over this period and also because it is the key region for SWV in terms of its impact on stratospheric temperatures and radiative forcing (Maycock *et al.*, 2011; Solomon *et al.*, 2010).

For the first time, observed latitude- and height-resolved SWV trends are imposed in a comprehensive GCM. Three case studies are investigated: the net increase between 1980 and 2010, the rapid decrease in the tropical lower stratosphere after 2000 and the wintertime dehydration in the Antarctic lower stratosphere. All of these cases have been documented in the literature (Nedoluha *et al.*, 2000; Rosenlof, 2001; Randel *et al.*, 2006; Scherer *et al.*, 2008; Hurst *et al.*, 2011) and showcase the differing mechanisms through which SWV changes can impact on temperature trends, as well as including both tropical and extratropical variations.

To quantify the long-term trend, we use the latest analysis of the Boulder frost-point hygrometer dataset from balloon sondes (the longest continuous record of SWV measurements) by Hurst *et al.* (2011), which resolves SWV variations in altitude and time at a point location (40°N, 105°W). To characterize shorter time-scale SWV variations, we use data from the Halogen Occultation Experiment (HALOE version 19) and Aura Microwave Limb Sounder (MLS version 2) satellite datasets. These datasets have been extensively validated in the literature (Harries *et al.*, 1996; Lambert *et al.*, 2007). HALOE data are adjusted to match the MLS values using latitude- and height-dependent offsets calculated from coincident observations taken during instrument overlap periods. However, these offsets do not impact on our experimental design, since we are primarily concerned with water vapour anomalies rather than absolute values on either interannual or seasonal time-scales. For the post-2000 case, the dataset used to design our model experiment primarily consists of HALOE data, with some MLS data included in the period 2004–2005. We will show that the water vapour decrease in the combined HALOE/MLS dataset compares very well with a previous estimate based on HALOE data alone. The dataset used to characterize the seasonal dehydration in the Antarctic consists only of MLS data for the period 2005–2009.

The remainder of the article is laid out as follows: Section 2 describes the comprehensive GCM and the set-up of the model experiments, section 3 describes the experiments carried out and presents our results and section 4 summarizes our findings in the context of their implications for observed stratospheric temperature trends.

2. Method

This study presents sensitivity experiments designed to test the impact of changes in SWV on stratospheric temperatures in a comprehensive stratosphere-resolving atmospheric GCM. The GCM is the same as that used by Maycock *et al.* (2013) and is described in detail by Hardiman *et al.* (2010) and Osprey *et al.* (2010). Briefly, it is a 60 level version of the atmospheric component of the Hadley Centre Global Environmental Model 1 (HadGAM1) with an upper boundary at $\sim$84 km, which is run at *N*48 horizontal resolution ($\sim$2.5° latitude × 3.75° longitude). The GCM simulates a reasonable representation of the climatology and variability of the stratosphere (see the above articles and references therein for details).

HadGAM1 includes the Edwards and Slingo (1996) radiation code updated to use the correlated-*k* method for calculating transmittances (Cusack *et al.*, 1999). This code has been shown to systematically overestimate the stratospheric temperature response and radiative forcing due to changes in SWV compared with more detailed radiation codes (Forster *et al.*, 2011; Maycock and Shine, 2012). In this study, changes in SWV are only imposed in the lower stratosphere, where the radiation code is associated with errors in the temperature change due to SWV perturbations of $\sim$30% for midlatitude summer and sub-Arctic winter conditions and $\sim$15% for tropical conditions (Maycock and Shine, 2012). All of the results presented in section 3 have therefore been scaled down by 30% to account for the known errors in the GCM's radiation code. However, since the error for tropical conditions has been estimated to be smaller than this, our results will be a conservative estimate of what the 'real world' response would be to an identical water vapour perturbation in the Tropics.

Each case study consists of a reference experiment, without any changes in SWV, and a perturbed experiment, with a fixed-in-time SWV perturbation imposed for the duration of each simulation. The SWV perturbations are included in the GCM by artificially modifying the water vapour field passed into the radiation code only above the lapse-rate tropopause, which is diagnosed using the WMO (1957) lapse-rate definition at each radiation timestep. For reference, the three pairs of experiments presented in this study and the SWV distributions prescribed in each of them are listed in Table 1. Following Maycock *et al.* (2013), each reference and perturbed experiment consists of a three-member ensemble run for 23 years from January 1980–December 2002, giving a total of 69 years of data. The simulations include time-varying concentrations of carbon dioxide, methane, nitrous oxide and chlorofluorocarbons. Volcanic aerosols are not included in any of the simulations.

The model is forced with monthly mean sea-surface temperatures (SSTs) and sea-ice concentrations taken from the Met Office Hadley Centre's SST and sea-ice dataset (HadISST: Rayner *et al.*, 2003). The use of time-varying SSTs and sea ice means that there is a more realistic signal-to-noise relationship in the experiments, as well as enabling the effects of the SWV perturbations to be isolated from other sources of stratospheric temperature variability, such as the El Niño Southern Oscillation (ENSO). However, the use of non-interactive SSTs means that the radiative impact of the imposed changes in SWV on surface temperatures will not be fully captured in the experiments. Ozone is prescribed as a zonal-mean monthly mean climatology from merged satellite datasets averaged over the period 1979–2003 (see Dall'Amico *et al.*, 2010 for further details). The effects of SWV perturbations on stratospheric chemistry are therefore not included in the simulations; however, some of the possible feedbacks are discussed later in section 3.3.

Note that in all of the experiments the changes in SWV are imposed as fixed-in-time perturbations, rather than time-varying trends. The model set-up is therefore effectively a time-slice configuration, with the exception of having time-varying SSTs, sea ice and long-lived greenhouse gas concentrations. It is therefore not reasonable to compare the temporal evolution of the simulated temperature changes with observations, but rather the focus here is on the implied net temperature changes due to the SWV perturbations over specified time periods.

Table 1. Description of the stratospheric water vapour fields for each of the three pairs of control and perturbed experiments discussed in this article. In all cases, the water vapour below the lapse rate tropopause is left as the model's own self-consistent free running tracer field.

		Corresponding stratospheric water vapour distribution
Exp 1	ORIG	Model's own simulated stratospheric water vapour field.
	TREND	As ORIG, but with 1980–2010 trend from Hurst *et al.* (2011) added as a constant-in-time height-dependent perturbation at all latitudes (see Table 2).
Exp 2	ORIG	As above.
	TROP	As ORIG, but with post-2000 SWV decrease based on the combined HALOE/MLS dataset added as a constant-in-time perturbation (see Figure 5(b)).
Exp 3	CTL	Constant fixed 3 ppmv at all latitudes/altitudes above the tropopause.
	DEHYD	As CTL, but with seasonal stratospheric Antarctic dehydration based on Aura MLS data included from June–December.

3. Results

3.1. Multi-decadal variations in SWV: the 1980–2010 trend

Hurst *et al.* (2011) present an updated analysis of the frost-point hygrometer record of SWV measurements taken at Boulder, Colorado. They provide estimates of the net change in SWV between March 1980 and January 2010 in 2 km layers for the altitude range 16–28 km; for reference, these trends are reproduced in Table 2, along with their 95% confidence intervals. It is important to note that this ∼30 year period includes the net positive trend between 1980 and 2000, the rapid decrease after 2000 and the more gradual recovery to pre-2000 concentrations in recent years (see Figure 4 of Hurst *et al.*, 2011). Although there are relatively large uncertainties in the trends, with the typical 95% confidence intervals being ∼25% of the mean, for the purposes of our experiments we assume that the best estimate is representative of 'truth'. This seems reasonable, since we must make further, larger assumptions about the behaviour of SWV as described below.

The SWV changes in Table 2 were added at all latitudes as a fixed-in-time perturbation to the model's time-evolving SWV field, using the method described in section 2. We therefore make the large assumption that these single point measurements can be considered globally representative. We justify this approximation because the available *in situ* and satellite data suggest that a net positive SWV trend was also observed across much of the globe during this period (Rosenlof, 2001; Smith *et al.*, 2001), albeit with large year-to-year variability. Since Hurst *et al.* (2011) do not provide estimates of the SWV trend for altitudes less than 16 km, we make the further assumption that the value in the lowest layer (16–18 km) is representative of the trend at all altitudes down to the local tropopause. Given the known mechanisms for water vapour transport in the stratosphere, it is very unlikely that SWV trends in the altitude range 16–28 km would occur in isolation from the layers above and below, and there is some observational evidence that our assumption is reasonable (Fujiwara *et al.*, 2010). However, no changes in SWV are imposed above 28 km in our experiment. This is mainly because, as described in section 1, it is changes in lower stratospheric water vapour that have the greatest impact on both stratospheric and tropospheric temperatures, but also because the Boulder measurements do not extend into the upper stratosphere. SWV perturbations in the upper stratosphere have been shown to have a considerably smaller impact on local temperature and global radiative forcing than equivalent changes in the lower stratosphere (Maycock *et al.*, 2011; Solomon *et al.*, 2010). Nevertheless, SWV trends at altitudes greater than 28 km are likely to be comparable to, or greater than, those in the range 16–28 km because of the larger contribution of methane oxidation in the upper stratosphere. The model set-up described above is referred to as the 'TREND' experiment. The baseline experiment without any imposed changes in SWV is denoted as 'ORIG'.

Figure 1 shows the differences in zonal-mean seasonal-mean temperature ($\overline{T}$) between the TREND and ORIG experiments expressed in terms of an effective trend (K decade^{-1}) for (a) June–August (JJA) and (b) December–February (DJF) seasons. The grey shading indicates where the differences are found to be statistically significant at the 95% confidence level using a two-tailed Student's t-test.* As expected, the increase in SWV causes cooling in the lower stratosphere. At a given pressure level, the cooling at high latitudes is generally larger than in the Tropics, which is consistent with the extratropical enhancement of the cooling due to SWV found in other studies (Forster and Shine, 1999; Maycock *et al.*, 2011). The peak magnitude of the cooling tendency is ∼0.1–0.2 K decade^{-1} in the Tropics and ∼0.2–0.3 K decade^{-1} in the extratropical and polar regions. The main exception to this is in the Northern Hemisphere (NH) extratropics in DJF, where the cooling reaches ∼0.5 K decade^{-1} over the Pole. There is also a statistically significant warming of similar magnitude in the uppermost stratosphere and lower mesosphere (0.2–5 hPa). We performed fixed dynamical heating calculations (using the method of Fels *et al.*, 1980, not shown), which show that this warming cannot be explained by radiative effects alone. This indicates that there is a dynamical response to the imposed SWV perturbation in the NH winter polar stratosphere. This is confirmed by analysis of the Transformed Eulerian Mean mass circulation in the stratosphere (Andrews *et al.*, 1987, not shown), which shows increased downwelling motion (adiabatic warming) in the upper stratosphere and decreased downwelling (adiabatic cooling) in the lower stratosphere. This is qualitatively consistent with the response to an increase in SWV in the lower stratosphere found by Maycock *et al.* (2013, see their Figure 8). However, the precise magnitude of the dynamical modification of the temperature change is subject to some uncertainty, given the relatively simple correction we have made to account for the known errors in the radiation code (see section 2).

Figure 2 shows the seasonal cycle of the effective temperature trend (K decade^{-1}) due to the increase in SWV as a function of latitude (ϕ) at 50 hPa. In the Tropics, the magnitude of the cooling trend is ∼0.1–0.25 K decade^{-1} throughout the year. In the Southern Hemisphere (SH) extratropics, the cooling trend is ∼0.2–0.3 K decade^{-1} from December–July; however, there are no statistically significant changes at southern high latitudes from August–November. In the NH extratropics, the cooling trend is ∼0.1–0.2 K decade^{-1} from May–October. In boreal winter, there is the suggestion of enhanced cooling at high northern latitudes. Although this is not statistically significant in the monthly mean data, it is a robust signal in the DJF mean (see Figure 1).

Figure 3 shows vertical profiles of the TREND-ORIG annual-mean $\overline{T}$ change (K decade^{-1}) averaged over (a) the globe, (b) 30°S–30°N, (c) 60–90°N and (d) 60–90°S. In all regions

*The Student's t-test is computed using the $3 \times 23 = 69$ years of data from each experiment, giving a combined sample size of 138.

Table 2. Values of the net change in stratospheric water vapour (ppmv) in 2 km layers between March 1980 and January 2010 from the Boulder frost-point hygrometer dataset and reproduced from Hurst *et al.* (2011). The values in brackets denote the 95% confidence limits.

	Altitude interval				
	16–18 km	18–20 km	20–22 km	22–24 km	24–26 km
1980–2010 SWV trend (ppmv)	0.71 (0.26)	0.80 (0.24)	1.12 (0.25)	1.25 (0.23)	1.20 (0.19)

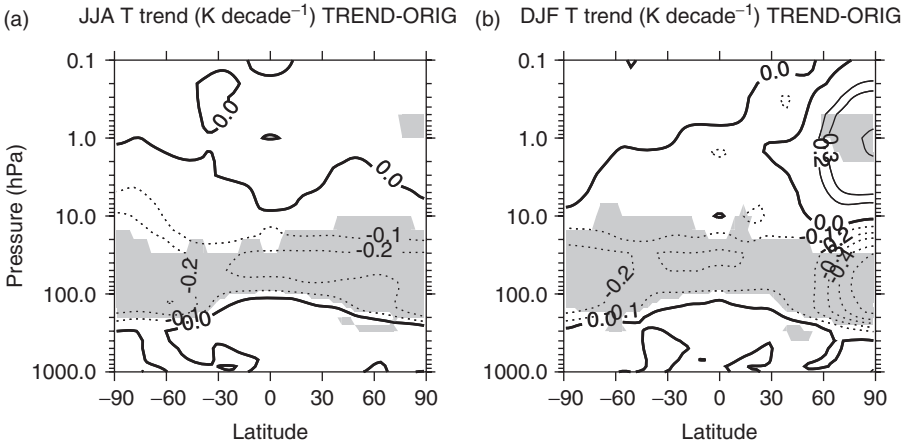

Figure 1. The $\overline{T}$ trend (K decade^{-1}) due to the change in SWV between 1980 and 2010 shown in Table 2 calculated from the difference between the TREND and ORIG experiments for (a) JJA and (b) DJF. The contour interval is 0.1 K decade^{-1}. The thick solid contour denotes the zero line. The shading indicates the regions where the differences are statistically significant at the 95% confidence level. Note that the differences shown in all plots have been scaled down by 30% to account for the known errors for SWV in the GCM radiation code.

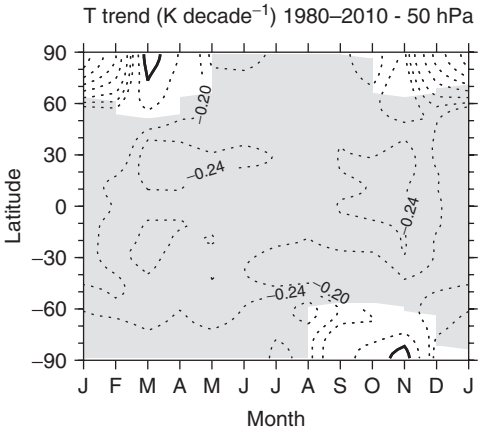

Figure 2. Latitude–time plot of the simulated temperature trend (K decade^{-1}) at 50 hPa due to the imposed 1980–2010 SWV trend. The shading indicates where the differences are statistically significant at the 95% confidence level. The contour interval is 0.1 K decade^{-1}. An additional contour is plotted at −0.24 K decade^{-1} to highlight the changes in the Tropics. The thick solid contour denotes the zero line.

considered, the cooling trend due to the change in SWV has a peak magnitude of 0.20–0.25 K decade^{-1}. In the global mean, there is a cooling trend between 10 and 200 hPa, which is largest in the layer 30–50 hPa. In the extratropics, the peak cooling extends from 30–150 hPa because of the lower height of the tropopause.

We now compare our model results with estimates of the observed temperature trend over this period. The black line in Figure 4 shows the temperature differences from Figure 3(a) weighted by the Microwave Sounding Unit (MSU) Temperature Lower Stratosphere (TLS) weighting function. This weighting function peaks at ∼17 km and samples in the altitude range 10–30 km, so it is appropriate for investigating the impact of lower stratospheric water vapour changes. The dashed lines show $\pm 2\sigma$ of the interannual variability from the model to give an estimate of the uncertainty in the inferred temperature trend. The grey line is the observed MSU TLS trend for the period 1979–2009 reproduced from Figure 8 of Seidel *et al.* (2011). For the MSU data, the dashed lines show the $\pm 2\sigma$ estimates due to the internal data uncertainties (Mears *et al.*, 2011). Note, however, that this does not reflect the uncertainty in the estimated linear trend itself. The total uncertainty is therefore larger than that shown here, particularly at high latitudes in winter when there is considerable year-to-year variability (see Figure 9 of Seidel *et al.*, 2011) and we therefore exclude these regions from our comparison.

The observed MSU TLS cooling trend is ∼0.3 K decade^{-1} in the Tropics and subtropics. Figure 4 shows that the trend in SWV could have contributed up to 30–40% of this cooling. Our experiment also suggests that the SWV trend could have had a larger impact on high-latitude wintertime temperatures, but as noted above the observed trends in these regions are currently less well constrained. Randel *et al.* (2009b) estimated a global mean annual mean lower stratospheric cooling trend of ∼0.5 K decade^{-1} between 1979 and 2007 using data from a number of satellite instruments and radiosonde databases. Figure 3(a) indicates that the SWV trend could have contributed up to 40–50% of the global mean cooling trend.

These results reinforce the conclusion of earlier studies that water vapour makes an important contribution to the radiative budget of the lower stratosphere and changes in its concentration can play a key role in determining temperature trends in this region (Shine *et al.*, 2003).

3.2. *Decadal variations in SWV: the rapid decrease after 2000*

The rapid decrease in tropical SWV after 2000 was observed in several satellite and *in situ* measurement datasets (Solomon *et al.*, 2010), and has been linked to changes in the strength of the Brewer–Dobson circulation (Randel *et al.*, 2006) and variations in tropical west Pacific SSTs (Rosenlof and Reid, 2008). The drop in SWV persisted for several years, although concentrations have now virtually returned to pre-2000 levels (Hurst *et al.*, 2011).

Figure 5(a) shows the difference in the annual-mean specific humidity (ppmv) between the four-year periods June 2001–May 2005 and January 1996–December 1999 calculated from the combined HALOE/MLS dataset. This is very similar to the equivalent calculation by Solomon *et al.* (2010) using HALOE data (see their Figure 1(b)). There was a decrease in water vapour over much of the stratosphere after 2000, with a peak reduction of ∼0.5 ppmv in the tropical lower stratosphere between 15°S

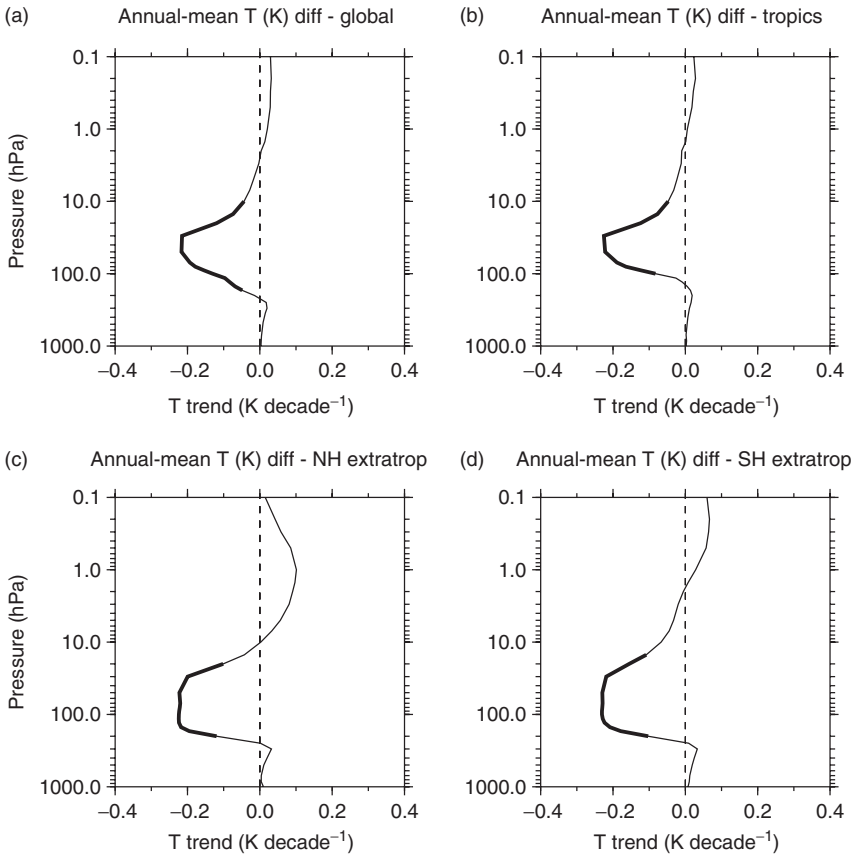

Figure 3. Vertical profiles of the annual-mean $\overline{T}$ trend (K decade^{-1}) for the TREND experiment averaged over (a) the globe, (b) the Tropics (30°N–30°S), (c) the Northern Hemisphere extratropics (60–90°N) and (d) the Southern Hemisphere extratropics (60–90°S). The thick lines denote where the differences are statistically significant at the 95% confidence level.

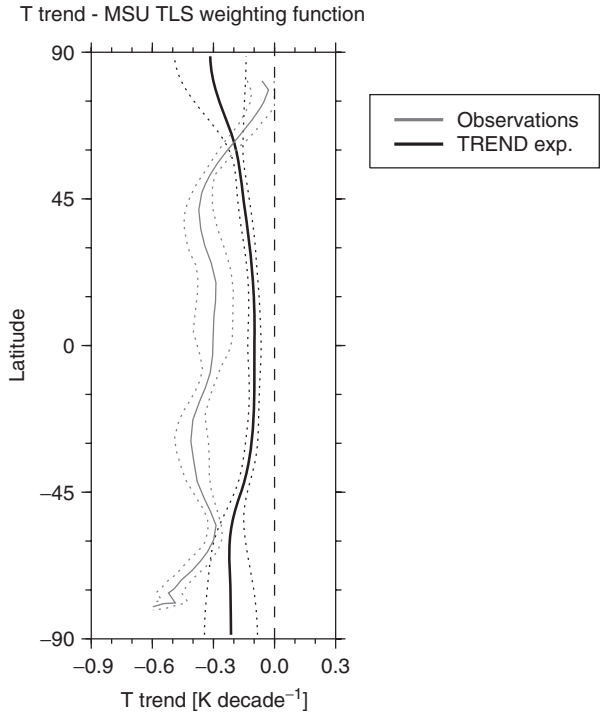

Figure 4. The latitudinal distribution of the annual-mean $\overline{T}$ trend (K decade^{-1}) for the TREND experiment weighted by the MSU TLS weighting function (black) and the observations for the period 1979–2009 reproduced from Seidel *et al.* (2011) (grey). The dotted lines denote the $\pm 2\sigma$ limits and the dashed line denotes the zero trend line.

and 15°N. It has been suggested that the radiative forcing due to the decrease in SWV may have contributed to decadal variability in global mean surface temperature (Solomon *et al.*, 2010). In addition, such a change would also be expected to impact on tropical lower stratosphere temperatures, and it is this effect that we consider here.

Figure 5(b) shows an analytic function designed to be an approximate representation of the observed change in SWV shown in Figure 5(a). The three-member ensemble experiment was repeated with the SWV anomaly in Figure 5(b) added as a fixed-in-time perturbation to the model's time-evolving water vapour field. This experiment is referred to as 'TROP'.

Figure 6 shows the seasonal-mean absolute differences in $\overline{T}$ (K) between the TROP and ORIG experiments for (a) JJA and (b) DJF. The decrease in SWV causes a relative increase in tropical lower stratospheric temperatures by up to 0.3 K at ∼60–70 hPa. The amplitude of the change in $\overline{T}$ decreases with increasing latitude and height, but the signal extends out to around $|\phi|$=60° in both hemispheres. Since the effect of the change in SWV on lower stratospheric temperature is small and positive, which would imply a weak negative feedback on water vapour transport into the stratosphere, the persistence of the post-2000 episode is likely to be related to changes in the tropical tropopause layer that are unrelated to the SWV evolution (i.e. SWV is responding to a temperature change forced by dynamical changes, e.g. Randel *et al.*, 2006; Rosenlof and Reid, 2008). Note that other changes that have been associated with the post-2000 episode, including increased tropical upwelling and decreased ozone concentrations (Randel *et al.*, 2006), would induce a cooling of the tropical lower stratosphere. There is no evidence of there being a detectable change in zonal winds in the GCM due to the imposed SWV perturbation (not shown).

Figure 7 shows the vertical profile of the annual-mean $\overline{T}$ difference (K) between the TROP and ORIG experiments averaged over 30°S–30°N. The change in SWV has the largest impact on tropical temperatures at ∼50 hPa, which coincides with the peak of the SWV perturbation as shown in Figure 5(b). The magnitude of the temperature change decreases rapidly with altitude above

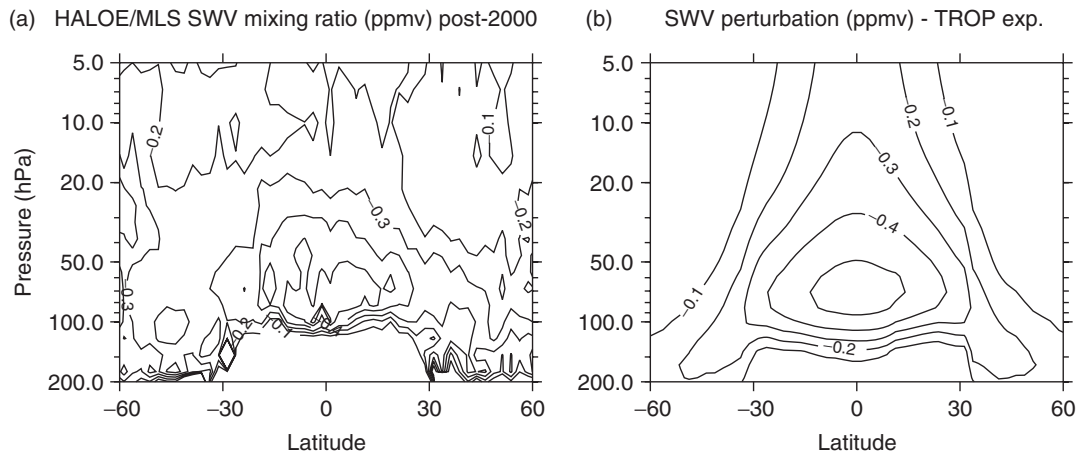

Figure 5. (a) The difference in SWV volume mixing ratio (ppmv) between the four-year periods June 2001–May 2005 and January 1996–December 1999 in the combined HALOE/MLS dataset. (b) The quasi-realistic SWV perturbation (ppmv) imposed in the TROP experiment. The contour interval is 0.1 ppmv. To highlight the region of interest, data are only shown for $-60^\circ \leq \phi \leq 60^\circ$ and 200–5 hPa.

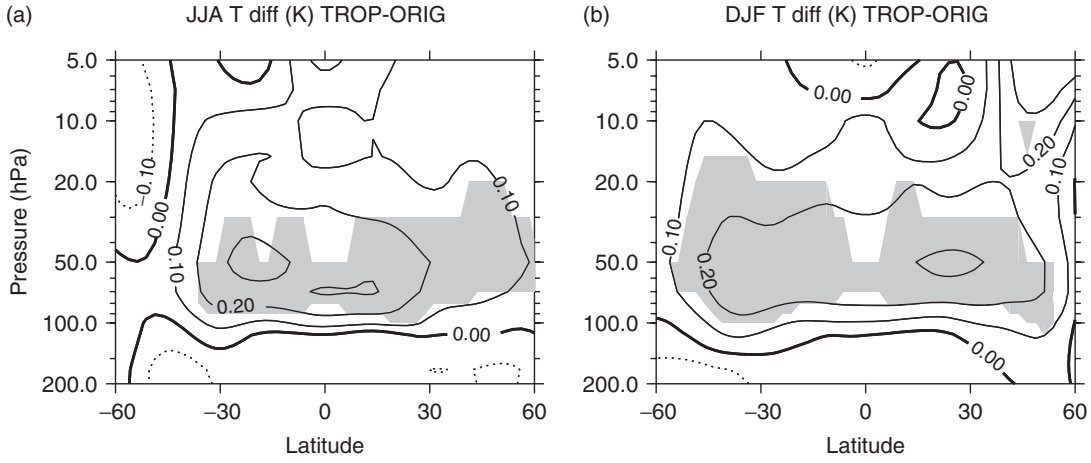

Figure 6. The differences between the TROP and ORIG experiments in $\overline{T}$ (K) for (a) JJA and (b) DJF seasons. The contour interval is 0.1 K. The thick solid contour denotes the zero line. The shading indicates where the differences are statistically significant at the 95% confidence level. The domain shown is the same as in Figure 5.

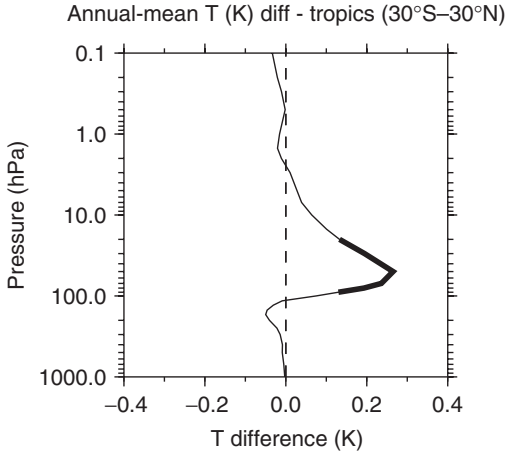

Figure 7. Vertical profile of the annual-mean difference in $\overline{T}$ (K) between the TROP and ORIG experiments averaged over the Tropics (30°N–30°S). The thick line denotes where the differences are statistically significant at the 95% confidence level.

and below this level, and there are no statistically significant changes outside the layer 20–100 hPa.

Although there was no apparent step-wise change in observed tropical lower stratospheric temperatures after the year 2000 (Randel *et al.*, 2009b), a signal of this magnitude and persistence may be hard to detect given the relatively large interannual variability in this region. Temperatures in this region are sensitive to many factors including ENSO (Randel *et al.*, 2009a), changes in the strength of tropical upwelling (Yulaeva *et al.*, 1994) and local ozone concentrations (Solomon *et al.*, 2012), which makes it difficult to separate the effect of SWV from other climatic drivers. However, our experiment shows that, all things being equal, the observed decrease in SWV would have raised tropical lower stratospheric temperatures by ∼0.3 K in the period 2001–2005.

3.3. Seasonal variations in SWV: dehydration in the Antarctic polar vortex

The formation of polar stratospheric ice clouds (type-II PSCs) can result in irreversible dehydration of the lower to mid stratosphere, since the ice particles sediment out and evaporate when they reach warmer air at lower altitudes (Vömel *et al.*, 1994). PSCs are more common in the Antarctic than in the Arctic, since the temperature at 80°S typically decreases to ∼185 K at 50 hPa in winter, compared with ∼202 K at 80°N (SPARC, 2002). Both *in situ* and satellite instruments have observed dehydration in the Antarctic stratospheric polar vortex (Vömel *et al.*, 1994; Nedoluha *et al.*, 2000). The formation of stratospheric clouds will impact directly on the local heating rate. The effect of a 100% coverage in type-II PSCs has been estimated to be an increase in the cooling rate of up to $\sim 0.2\,\mathrm{K\,day^{-1}}$ poleward of 75°S and a decrease of $\sim 0.2\,\mathrm{K\,day^{-1}}$ equatorward of 75°S (Hicke and Tuck, 2001). Here, we will not consider the direct effect of PSCs on stratospheric heating rates, but rather we focus on the impact of the dehydration itself on stratospheric temperatures, which to our knowledge has not been quantified previously. Although this seasonal dehydration is a climatological feature in the Antarctic (Ramaswamy, 1988; Vömel *et al.*, 1994), its magnitude and persistence could change as a result of stratospheric temperature

trends and/or SWV trends. It is therefore important to investigate the impact of dehydration on the stratosphere, since it has the potential to contribute to model biases and/or trends in polar temperatures.

Figure 8(a) shows the specific humidity at 100 hPa from MLS data averaged over the period 2005–2009. The seasonal cycle in the SH polar-cap average ($\phi > 60^\circ$S) SWV mixing ratio shows a peak change of −1.3 ppmv between April and September. This dehydration typically occurs in the altitude range ∼12–24 km (Nedoluha *et al.*, 2000). The values compare well with estimates of the dehydration derived from other data sources (see e.g. Figure 6.31 of SPARCCCMVal (2010) and Figure 3 of Nedoluha *et al.* (2000)). Figure 8(b) shows an analytic function designed to approximately capture the seasonal cycle in specific humidity in Figure 8(a). The wintertime anomalies have been defined relative to an idealized uniform summertime background concentration of 3 ppmv, and there is therefore a constant offset of ∼1 ppmv between the water vapour mixing ratios shown in Figure 8(a) and (b). However, the seasonal cycle of polar cap SWV for the analytic function shows a peak change of −1.1 ppmv, which compares well with the MLS data.

The three-member ensemble GCM experiment was repeated with the SWV distribution in Figure 8(b) imposed uniformly in the pressure range 30–190 hPa. Everywhere else and at all other times the SWV concentration takes a fixed value of 3 ppmv. This model set-up is referred to as the 'DEHYD' experiment. The reference experiment in this case, which is referred to as 'CTL', is therefore a simulation in which the water vapour concentration takes a constant fixed-in-time value of 3 ppmv everywhere in the stratosphere (see Maycock *et al.*, 2013, for more details).

Figure 9 shows the monthly mean differences in $\overline{T}$ (K) between the DEHYD and CTL experiments in the SH for July–December ((a)–(f)). Outside these months there are no statistically significant changes in temperature. The impact of the dehydration is first evident in July, when there is a relative warming of ∼0.5 K at $\phi > 75^\circ$S. This signal increases in magnitude over the winter and reaches a maximum of ∼1.1 K at $\phi > 80^\circ$S in September. The change in the polar-cap average $\overline{T}$ at 150 hPa is 0.4, 0.6 and 0.2 K in August, September and October, respectively. This is at least an order of magnitude smaller than the impact of ozone depletion on temperatures in the Antarctic stratosphere, which is estimated to have caused a relative cooling of ∼7 K at similar altitudes compared with pre-1970 conditions (Thompson and Solomon, 2002).

The relative warming over the polar cap shown in Figure 9 causes a slight weakening of the background westerlies on the poleward flank of the stratospheric jet (not shown). The decrease in zonal-mean zonal wind ($\bar{u}$) has a maximum amplitude of ∼1.5 m s^{-1} between 60 and 75°S and 5–50 hPa in September. The mean background wind in this region in the GCM ranges from ∼30–50 m s^{-1}, so this represents a deceleration of ∼2–5%. There are no significant changes in $\bar{u}$ from October–December. However, unlike the case of ozone depletion, which has resulted in a poleward shift in the tropospheric midlatitude jet in austral spring/summer in recent decades (Polvani *et al.*, 2011), there is no evidence of there being a change in the tropospheric circulation in response to the imposed Antarctic dehydration.

The impact of ozone depletion on stratospheric temperatures peaks in October–November (Thompson and Solomon, 2002). The largest changes in $\overline{T}$ in response to the dehydration are found in August–September in the GCM. The signal of dehydration in the Antarctic stratosphere therefore peaks several months earlier than that of ozone depletion. In addition to the effects on temperature, the dehydration could also impact on ozone depletion in austral spring, for example by altering chemical reaction rates and the availability of water vapour for chemical interactions. There is also the potential for a negative feedback not included in these simulations, since the effect of the dehydration is to increase stratospheric temperatures, which to first order would make type-II PSCs less likely to form.

4. Conclusions

This study has investigated the potential direct impact of observed changes in stratospheric water vapour (SWV) on stratospheric temperatures in a comprehensive global climate model (GCM). Three case studies for SWV have been investigated: the long-term net increase from 1980–2010, the rapid decrease in the tropical lower stratosphere after 2000 and the seasonal dehydration that occurs in the Antarctic stratospheric polar vortex.

The GCM's radiation code contains known biases in its representation of stratospheric water vapour (Maycock and Shine, 2012). We therefore scaled down the temperature changes simulated in the model by 30% to enable a fairer comparison with observations. This is the estimated magnitude of the difference in the fixed dynamical heating temperature change for SWV compared with a more detailed radiation code for midlatitude and extratropical conditions. However, the relative error was found to be smaller for tropical conditions (∼15%), which means that our results are likely to be a conservative estimate of what the 'real world' response would be to an identical water vapour perturbation in the Tropics.

The paucity of long-term continuous global measurements makes it challenging to quantify long-term changes in SWV and this issue has been discussed at length in the literature. Here we have used the estimated SWV trends in the altitude range 16–26 km over the period 1980–2010 provided by Hurst *et al.* (2011), which are derived from frost-point hygrometer measurements taken at Boulder, Colorado (40°N, 105°W). To quantify the contribution of long-term changes in SWV to stratospheric temperature trends using a GCM, we have made four key assumptions.

- The best estimates provided by Hurst *et al.* (2011) are representative of 'truth', i.e. we do not account for uncertainties in the trends, which amount to a 95% confidence interval of ∼25% of the mean value.
- The point measurements taken at Boulder are representative of global changes.
- The SWV change in the 16–18 km layer is representative of trends at all altitudes down to the local tropopause.
- The effect of SWV in isolation can be considered representative of its effect when a combination of forcings is present (e.g. changes in carbon dioxide, ozone and SWV).

With these caveats, the net increase in SWV from 1980–2010 is associated with a cooling of the lower stratosphere of up to 0.24 K decade^{-1} at 50 hPa in the annual and global mean. This is at the lower end of the estimated cooling trend due to SWV for the period 1980–2000 presented by Shine *et al.* (2003). Forster and Shine (1999) calculated a cooling trend of ∼0.4 K decade^{-1} at 50 hPa in the Tropics due to a globally uniform increase in SWV of 0.7 ppmv. This perturbation is comparable to that imposed in the TREND experiment (although theirs is not height-varying) and therefore the magnitude of the temperature trend calculated here is around a third smaller than that of Forster and Shine (1999), but within the range found in other studies (Shine *et al.*, 2003; Seidel *et al.*, 2011).

In the Arctic polar stratosphere, there is a dynamical response to the increase in SWV in wintertime, with increased downwelling (adiabatic warming) in the upper stratosphere and decreased downwelling (adiabatic cooling) in the lower stratosphere. This enhances the radiatively driven cooling in the lower stratosphere by around a factor of three and causes a relative warming of ∼0.5 K decade^{-1} in the upper stratosphere and lower mesosphere. This is qualitatively consistent with the dynamical response to an increase in lower stratospheric water vapour found by Maycock *et al.* (2013).

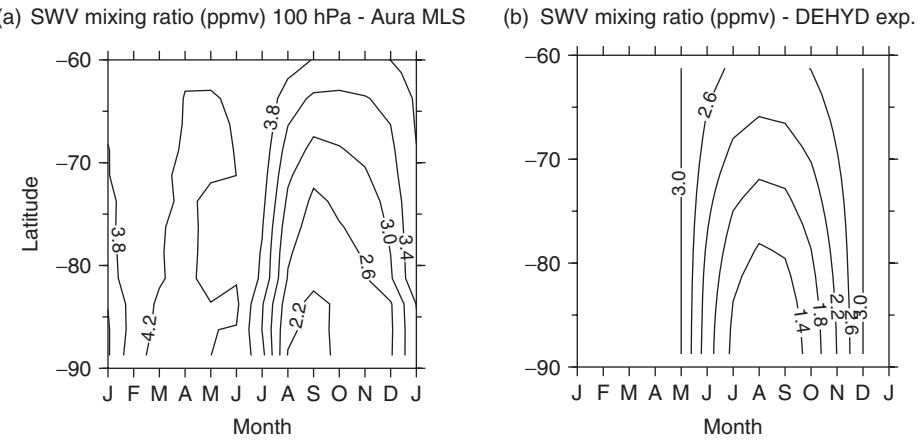

Figure 8. Latitude–time plots of the monthly mean SWV volume mixing ratio (ppmv) at 100 hPa for (a) Aura MLS data averaged over 2005–2009 and (b) the quasi-realistic SWV anomaly imposed in the DEHYD experiment. The contour interval in both panels is 0.4 ppmv.

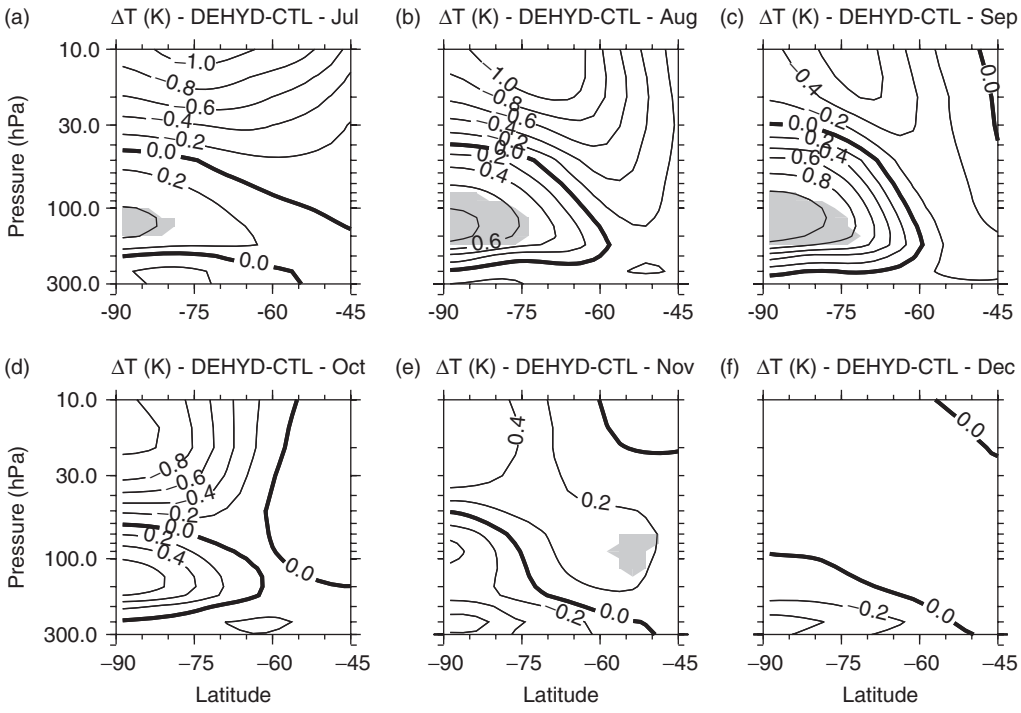

Figure 9. Plots of the monthly mean differences in $\overline{T}$ (K) between the DEHYD and CTL experiments for (a)–(f) July–December, respectively. The contour interval is 0.2 K. The thick solid contour denotes the zero line. The shading indicates where the differences are statistically significant at the 95% confidence level. To highlight the region of interest, data are only shown south of 45°S and in the pressure range 300–10 hPa.

Several *in situ* and satellite datasets suggest that there was a rapid decrease in tropical lower stratospheric water vapour of ∼15% after 2000 (Solomon *et al.*, 2010). Although there has been considerable interest in the radiative forcing associated with this change, its impact on stratospheric temperatures has not been previously quantified. We have shown that the decrease in SWV would have caused a relative warming of the tropical lower stratosphere by ∼0.3 K, which is roughly one third of the estimated cooling due to ozone depletion in this region over recent decades (Polvani and Solomon, 2012). It is important to note that there is the potential for a negative feedback to take place for tropical SWV perturbations, since a decrease in water vapour warms the tropopause region, which to first order would be expected to decrease the dehydration of air entering into the stratosphere.

The formation of ice clouds in the Antarctic polar vortex leads to irreversible dehydration of air in the altitude range ∼12–24 km. Past studies have considered the direct impact of polar stratospheric clouds (PSCs) on stratospheric heating rates, but to our knowledge the impact of the dehydration on temperatures has not been previously quantified. The relative change in polar-cap specific humidity at 100 hPa is −1.3 ppmv between April and September in Aura Microwave Limb Sounder (MLS) data. When imposed in the GCM, the observed wintertime dehydration causes a relative warming of the polar lower stratosphere from July–October by up to ∼1 K. This causes a slight weakening of the westerlies on the poleward flank of the stratospheric jet by up to 1.5 m s^{-1} in September. The impact of the dehydration on the stratosphere peaks 1–2 months earlier, but is considerably weaker than the effects of stratospheric ozone depletion.

In our simulations, none of the changes in SWV investigated had a detectable impact on the tropospheric circulation. This indicates that it is larger SWV trends, such as those simulated by some chemistry–climate models in response to increases in anthropogenic greenhouse gas emissions (Gettelman *et al.*, 2010), that are more likely to be important for stratospheric and tropospheric circulation patterns (Joshi *et al.*, 2006; Maycock *et al.*, 2013). However, the results presented here reinforce earlier studies, which demonstrate that observed changes in SWV could have made a significant contribution to the evolution of stratospheric temperatures (Shine *et al.*, 2003). With the caveat that the Boulder data have been assumed to be globally representative, our results show that SWV changes may have been

as important as carbon dioxide and ozone for driving global lower stratospheric temperature trends over the past three decades. It is therefore a priority that SWV should continue to be monitored in the future, so that its role in climate can be better understood and quantified.

Acknowledgements

ACM was supported by a NERC PhD studentship at the University of Reading and a CASE award from the UK Met Office. MMJ was funded by NCAS-Climate, which is a NERC funded research centre. The authors thank the three anonymous reviewers for their suggestions on how to improve the manuscript.

References

Andrews DG, Holton JR, Leovy CB. 1987. *Middle Atmosphere Dynamics* (1st edn). Academic Press: London.

Cusack S, Edwards JM, Crowther MJ. 1999. Investigating *k* distribution methods for parameterizing gaseous absorption in the Hadley Centre Climate Model. *J. Geophys. Res.* **104**: 2051–2057, doi: 10.1029/1998JD200063.

Dall'Amico M, Stott PA, Scaife AA, Gray LJ, Rosenlof KH, Karpechko AY. 2010. Impact of stratospheric variability on tropospheric climate change. *Clim. Dyn.* **34**: 399–417.

Edwards JM, Slingo A. 1996. Studies with a flexible new radiation code. I: Choosing a configuration for a large-scale model. *Q. J. R. Meteorol. Soc.* **122**: 689–719.

Fels SB, Mahlman JD, Schwarzkopf MD, Sinclair RW. 1980. Stratospheric sensitivity to perturbations in ozone and carbon dioxide: Radiative and dynamical response. *J. Atmos. Sci.* **37**: 2265–2297.

Forster PM, Shine KP. 1999. Stratospheric water vapour changes as a possible contributor to observed stratospheric cooling. *Geophys. Res. Lett.* **26**: 3309–3312, doi: 10.1029/1999GL010487.

Forster PM, Shine KP. 2002. Assessing the climate impacts of trends in stratospheric water vapour. *Geophys. Res. Lett.* **29**: 1086–1089, doi: 10.1029/2001GL013909.

Forster PM, Fomichev VI, Rozanov E, Cagnazzo C, Jonsson AI, Langematz U, Fomin B, Iacono MJ, Mayer B, Mlawer E, Myhre G, Portmann RW, Akiyoshi H, Falaleeva V, Gillett N, Karpechko A, Li J, Lemennais P, Morgenstern O, Oberländer S, Sigmond M, Shibata K. 2011. Evaluation of radiation scheme performance within chemistry-climate models. *J. Geophys. Res* **116**: D10302.

Fueglistaler S, Haynes P. 2005. Control of interannual and longer-term variability of stratospheric water vapor. *J. Geophys. Res.* **110**: D24108.

Fujiwara M, Vömel H, Hasebe F, Shiotani M, Ogino SY, Iwasaki S, Nishi N, Shibata T, Shimizu K, Nishimoto E, Valverde Canossa JM, Selkirk HB, Oltmans SJ. 2010. Seasonal to decadal variations of water vapor in the tropical lower stratosphere observed with balloon-borne cryogenic frost point hygrometers. *J. Geophys. Res.* **115**: D18304.

Gettelman A, Hegglin MI, Son SW, Kim J, Fujiwara M, Birner T, Kremser S, Rex M, Añel JA, Akiyoshi H, Austin J, Bekki S, Braesike P, Brühl C, Butchart N, Chipperfield M, Dameris M, Dhomse S, Garny H, Hardiman SC, Jöckel P, Kinnison DE, Lamarque JF, Mancini E, Marchand M, Michou M, Morgenstern O, Pawson S, Pitari G, Plummer D, Pyle JA, Rozanov E, Scinocca J, Shepherd TG, Shibata K, Smale D, Teyssèdre H, Tian W. 2010. Multimodel assessment of the upper troposphere and lower stratosphere: Tropics and global trends. *J. Geophys. Res.* **115**: D00M08.

Hardiman SC, Butchart N, Osprey SM, Gray LJ, Bushell AC, Hinton TJ. 2010. The climatology of the middle atmosphere in a vertically extended version of the Met Office's climate model. Part I: Mean state. *J. Atmos. Sci.* **67**: 1509–1525.

Harries JE, Russell JM, Tuck AF, Gordley LL, Purcell P, Stone K, Bevilacqua RM, Gunson M, Nedoluha G, Traub WA. 1996. Validation of measurements of water-vapour from the Halogen Occulation Experiment (HALOE). *J. Geophys. Res.* **101**: 10205–10216.

Hicke J, Tuck A. 2001. Polar stratospheric cloud impacts on Antarctic stratospheric heating rates. *Q. J. R. Meteorol. Soc.* **127**: 1645–1658.

Hurst DF, Oltmans SJ, Vömel H, Rosenlof KH, Davis SM, Ray EA, Hall EG, Jordan AF. 2011. Stratospheric water vapor trends over Boulder, Colorado: Analysis of the 30 year Boulder record. *J. Geophys. Res.* **116**: D02306, doi: 10.1029/2010JD015065.

Joshi MM, Charlton AJ, Scaife AA. 2006. On the influence of stratospheric water vapor changes on the tropospheric circulation. *Geophys. Res. Lett.* **33**: L09806, doi: 10.1029/2006GL025983.

Lambert A, Read WG, Livesey NJ, Santee ML, Manney GL, Froidevaux L, Wu DL, Schwartz MJ, Pumphrey HC, Jimenez C, Nedoluha GE, Cofield RE, Cuddy DT, Daffer WH, Drouin BJ, Fuller RA, Jarnot RF, Knosp BW, Pickett HM, Perun VS, Snyder WV, Stek PC, Thurstans RP, Wagner PA, Waters JW, Jucks KW, Toon GC, Stachnik RA, Bernath PF, Boone CD, Walker KA, Urban J, Murtagh D, Elkins JW, Atlas E. 2007. Validation of the Aura Microwave Limb Sounder middle atmosphere water vapor and nitrous oxide measurements. *J. Geophys. Res.* **112**: D24S36.

Le Texier H, Solomon S, Garcia RR. 1988. The role of molecular hydrogen and methane oxidation in the water vapour budget of the stratosphere. *Q. J. R. Meteorol. Soc.* **114**: 281–295.

Maycock AC, Shine KP. 2012. Stratospheric water vapour and climate: Sensitivity to the representation in radiation codes. *J. Geophys. Res.* **117**: D13102, doi: 10.1029/2012JD017484.

Maycock AC, Shine KP, Joshi MM. 2011. The temperature response to stratospheric water vapour changes. *Q. J. R. Meteorol. Soc.* **137**: 1070–1082.

Maycock AC, Joshi MM, Shine KP, Scaife AA. 2013. The circulation response to idealized changes in stratospheric water vapour. *J. Clim.* **26**: 545–561, doi: 10.1175/JCLI-D-12-00155.1.

Mears CA, Wentz FJ, Thorne P, Bernie D. 2011. Assessing uncertainty in estimates of atmospheric temperature changes from MSU and AMSU using a Monte-Carlo estimation technique. *J. Geophys. Res.* **116**: D08112.

Mote PW, Rosenlof KH, McIntyre ME, Carr ES, Gille JC, Holton JR, Kinnersley JS, Pumphrey HC, Russell JH III, Waters JW. 1996. An atmospheric tape recorder: The imprint of tropical tropopause temperatures on stratospheric water vapor. *J. Geophys. Res.* **101**: 3989–4006.

Nedoluha GE, Bevilacqua RM, Hoppel KW, Daehler M, Shettle EP, Hornstein JH, Fromm MD, Lumpe JD, Rosenfield JE. 2000. POAM III measurements of dehydration in the Antarctic lower stratosphere. *Geophys. Res. Lett.* **27**: 1683–1686, doi: 10.1029/1999GL011087.

Oinas V, Lacis AA, Rind D, Shindell DT, Hansen JE. 2001. Radiative cooling by stratospheric water vapor: Big differences in GCM results. *Geophys. Res. Lett.* **28**: 2791–2794, doi: 10.1029/2001GL013137.

Osprey SM, Gray LJ, Hardiman SC, Butchart N, Bushell AC, Hinton TJ. 2010. The climatology of the middle atmosphere in a vertically extended version of the Met Office's climate model. Part II: Variability. *J. Geophys. Res.* **67**: 3637–3651.

Polvani L, Solomon S. 2012. The signature of ozone depletion on tropical temperature trends, as revealed by their seasonal cycle in model integrations with single forcings. *J. Geophys. Res.* **117**: D17102.

Polvani LM, Waugh DW, Correa GJP, Son SW. 2011. Stratospheric ozone depletion: The main driver of 20th Century atmospheric circulation changes in the Southern Hemisphere. *J. Clim.* **24**: 795–812.

Ramaswamy V. 1988. Dehydration mechanism in the Antartic during winter. *Geophys. Res. Lett.* **15**: 863–866, doi: 10.1029/GL015i008p00863.

Randel WJ, Wu F, Vömel H, Nedoluha GE, Forster PM. 2006. Decreases in stratospheric water vapor after 2001: Links to changes in the tropical tropopause and the Brewer–Dobson circulation. *J. Geophys. Res.* **111**: D12312.

Randel WJ, Garcia RR, Calvo N, Marsh D. 2009a. ENSO influence on zonal mean temperature and ozone in the tropical lower stratosphere. *Geophys. Res. Lett.* **36**: L15822, doi: 10.1029/2009GL039343.

Randel WJ, Shine KP, Austin J, Barnett J, Claud C, Gillett NP, Keckhut P, Langematz U, Lin R, Long C, Mears C, Miller A, Nash J, Seidel DJ, Thompson DWJ, Wu F, Yoden S. 2009b. An update of observed stratospheric temperature trends. *J. Geophys. Res.* **114**: D02107.

Rayner NA, Parker DE, Horton EB, Folland CK, Alexander LV, Rowell DP, Kent EC, Kaplan A. 2003. Global analyses of sea surface temperature, sea ice, and night marine air temperature since the late nineteenth century. *J. Geophys. Res.* **108**: 4407–4435.

Rosenlof KH, Oltmans SJ, Kley D, Russell III JM, Chiou E-W, Chu WP, Johnson DG, Kelly KK, Michelsen HA, Nedoluha GE, Remsberg EE, Toon GC, McCormick MP. 2001. Stratospheric water vapour increases over the past half century. *Geophys. Res. Lett.* **28**: 1195–1198, doi: 10.1029/2000GL012502.

Rosenlof KH, Reid GC. 2008. Trends in the temperature and water vapor content of the tropical lower stratosphere: Sea surface connection. *J. Geophys. Res.* **113**: D06107, doi: 10.1029/2007JD009109.

Scherer M, Vömel H, Fueglistaler S, Oltmans SJ, Stähelin J. 2008. Trends and variability of midlatitude stratospheric water vapour deduced from the re-evaluated boulder balloon series and HALOE. *Atmos. Chem. Phys.* **8**: 1391–1402.

Seidel DJ, Gillett NP, Lanzante JR, Shine KP, Thorne PW. 2011. Stratospheric temperature trends: Our evolving understanding. *Wiley Interdiscip. Rev. Clim. Change* **2**: 592–616.

Shine KP, Bourqui MS, Forster PMD, Hare SHE, Langematz U, Braesicke P, Grewe V, Ponater M, Schnadt C, Smith CA, Haigh JD, Austin J, Butchart N, Shindell DT, Randel WJ, Nagashima T, Portmann RW, Solomon S, Seidel DJ, Lanzante J, Klein S, Ramaswamy V, Schwarzkopf MD. 2003. A comparison of model-simulated trends in stratospheric temperatures. *Q. J. R. Meteorol. Soc.* **129**: 1565–1588.

Smith CA, Haigh JD, Toumi R. 2001. Radiative forcing due to trends in stratospheric water vapour. *Geophys. Res. Lett.* **28**: 179–182, doi: 10.1029/2000GL011846.

Solomon S, Rosenlof KH, Portmann R, Daniel J, Davis S, Sanford T, Plattner GK. 2010. Contributions of stratospheric water vapor changes to decadal variation in the rate of global warming. *Science* **327**: 1219–1222.

Solomon S, Young PJ, Hassler B. 2012. Uncertainties in the evolution of stratospheric ozone and implications for recent temperature changes in the tropical lower stratosphere. *Geophys. Res. Lett.* **39**: L17706, doi: 10.1029/2012GL052723.

SPARC. 2002. SPARC Intercomparison of Middle Atmosphere Climatologies, SPARC Report 3, WCRP-116, WMO/TD-No. 1142, Randel W, Chanin

M-L, Michaut C (eds.). http://www.sparc-climate.org/publications/sparc-reports/.

SPARC CCMVal. 2010. SPARC Report on the Evaluation of Chemistry–Climate Models, SPARC Report 5, WCRP-132, WMO/TD-No. 1526, Eyring V, Shepherd TG, Waugh D (eds.). http://www.sparc-climate.org/publications/sparc-reports/.

Thompson DWJ, Solomon S. 2002. Interpretation of recent Southern Hemisphere climate change. *Science* **296**: 895–899.

Vömel H, Oltmans SJ, Hofmann DJ, Deshler T, Rosen JM. 1994. The evolution of the dehydration in the Antarctic stratospheric vortex. *J. Geophys. Res.* **100**: 13919–13926.

World Meteorological Organization (WMO). 1957. Meteorology – A three-dimensional science: Second session of the Commission for Aerology, WMO Bulletin IV (4). WMO: Geneva, Switzerland.

Yulaeva E, Holton JR, Wallace JM. 1994. On the cause of the annual cycle in tropical lower-stratospheric temperatures. *J. Atmos. Sci.* **51**: 169–174.